



Analysis of the mechanical response of film on substrate systems presenting rough interfaces

Hervé Bordet, Michel Ignat^{*}, Michel Dupeux

Laboratoire de Thermodynamique et de Physico-Chimie Métallurgiques, (CNRS UMR 5614-INPG / UJF) E.N.S.E.E.G., BP. 75, 38402 Saint Martin d'Hères, France

Received 28 May 1997; accepted 3 September 1997

Abstract

The effect of the mechanical polishing of the substrate surface on which thin films were deposited was investigated by 'in situ' tensile tests. These tests, performed in a Scanning Electron Microscope, showed different responses through cracking and debonding behaviour of the films, which could be related to the roughness of the substrate surfaces fixed by the granulometry of the polishing paste. The rougher surfaces produced an activation of film cracking and debonding earlier than the smoother ones. We also observed that the crack activation was dependent on the direction of the scratches which were produced before the deposition on the samples surfaces. Two directions of scratches were investigated, perpendicular and parallel to the sample tensile axis. A simple energy balance gave apparent values of the critical cracking energy of the film/substrate interfaces. © 1998 Elsevier Science S.A.

Keywords: Adhesion; Interfaces; Monolayers; Silicon oxide; Surface roughness

1. Introduction

One of the important intrinsic parameters, which will act on the mechanical stability of film on substrate systems, concerns the microscopic scale irregularities of the interface geometry. At nanoscopic scales, the effect of the interface roughness on the thin film growth has been analysed, for example in the case of heteroepitaxial grown films.

At microscopic and higher scales, and for film or coatings which present amorphous or polycrystalline microstructures, the interfacial roughness effect is often detected indirectly. Indeed, in certain circumstances, the modification of the physical or chemical parameters used for cleaning the substrate surface prior to the deposition of the films appear to act upon the global mechanical response of the system, suppressing or promoting damage mechanisms.

A substantial theoretical and experimental background relevant to brittle films deposited on ductile substrates is available in the literature, and provides information on the mechanical behaviour of such film on substrate systems

(see for instance Refs. [1–4]). For example the effect of a rough surface on the adhesion of mica surfaces was analysed by Tabor [5]. It was shown then that the adhesion depends not only on the surface forces, but also on the roughness of the interface and on the mechanical properties of the solids. Chan [6] investigated the possible relationship between crack deflection, surface roughness and fracture toughness, by considering the toughening effects in two phase TiAl alloys. Savage et al. [7] analysed the interfacial roughness with respect to the films thickness and the period of W/C multilayers deposited on Si substrates. The relation between interfacial roughness and film growth was studied by Jero and Kerans [8] for glass matrix composites.

The aim of the present work is to investigate the influence of an interfacial roughness on the evolution of damage of SiO₂ thin films deposited on Al–Si substrates. We prepared microtensile samples of the film on substrate systems, with different mechanical polishings of the substrate surface, but with the same deposition conditions for all films. The samples were tested in tension to determine the experimental conditions required to produce cracking and debonding of the films. This behaviour was then related to the roughness of the interfaces and discussed with respect to it.

^{*} Corresponding author.

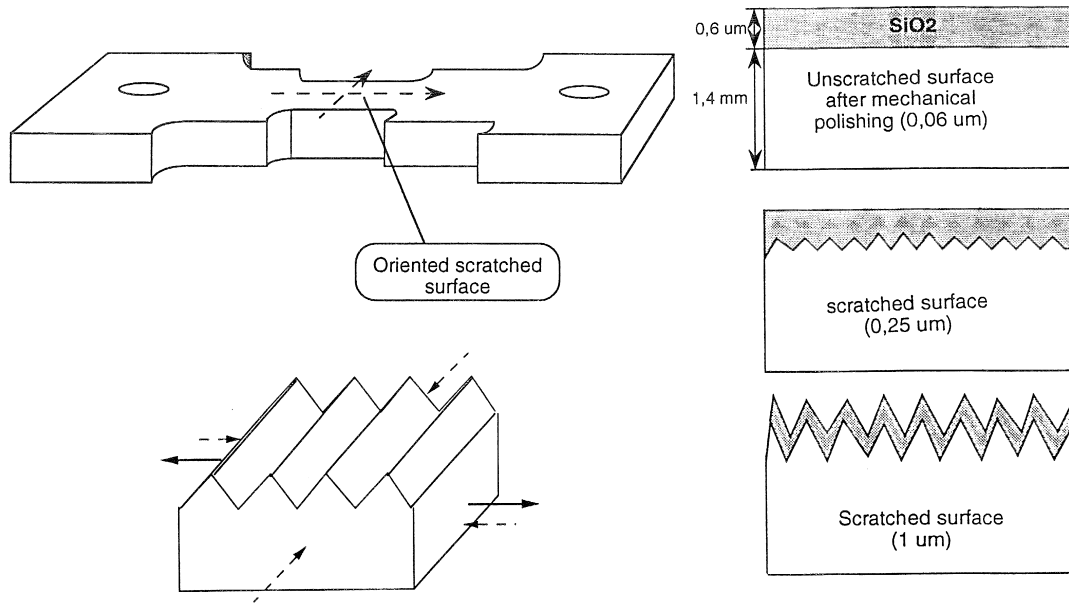


Fig. 1. (a) Schematic view of the tensile specimen; The dotted lines correspond to the polishing directions. (b) Film on substrate systems investigated in the present work. (c) Schematic view of the stress state in the film; dotted arrows represent the residual compressive equi-biaxial stresses and full arrows the applied tensile stress.

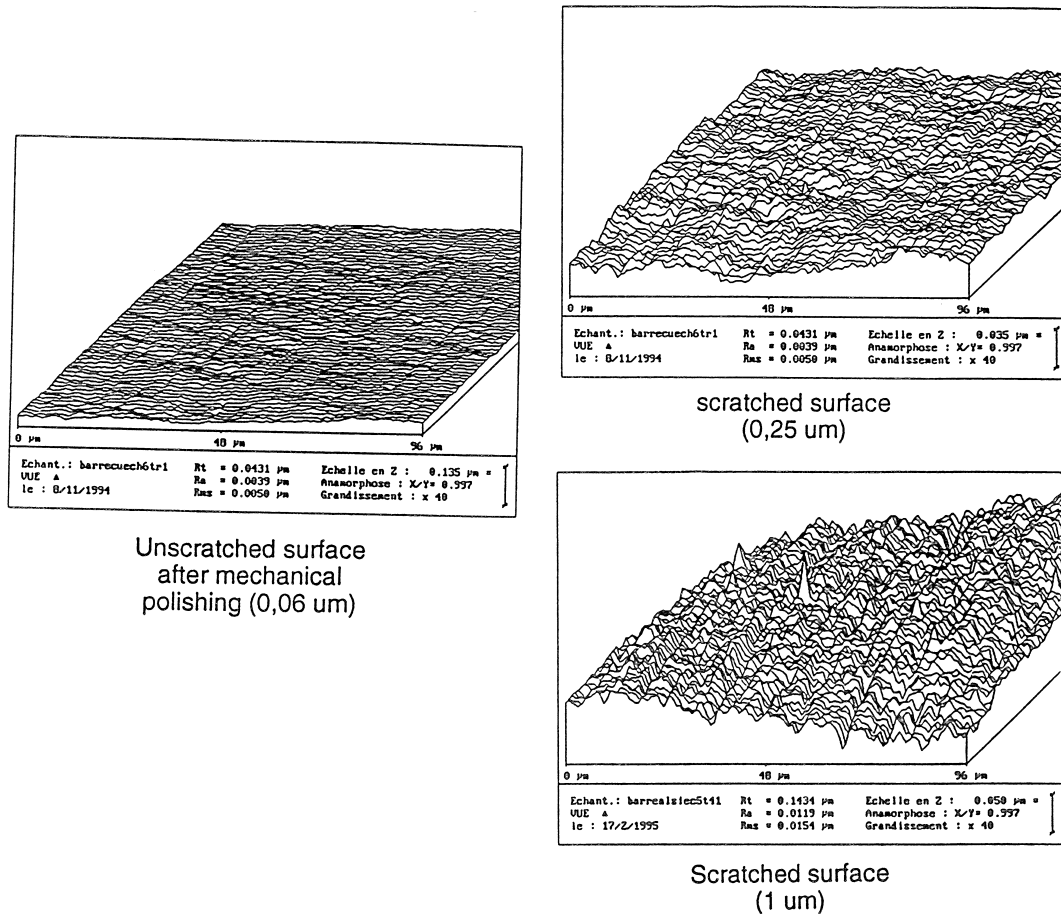


Fig. 2. Induced roughness on the substrate surface before film deposition (3D optical interferometry surface profiles); the average Rms roughness is indicated on the labels.

2. Experimental

Our purpose was to investigate the behaviour under tensile stress of film/substrate systems which present variable interfacial roughness both in amplitude and in direction, obtained by mechanical polishing. We chose a system for which the substrate would allow enough strain transfer (aluminium based solid solutions), and a film of SiO_2 which is a well known material for microelectronic applications and has much less ability to strain plastically than the substrate. Consequently, increasing strain of the substrate (elastic then plastic) will induce irreversible damage to the film, first cracking transverse to the tensile direction, then decohesion from the substrate and spalling.

2.1. Preparation of the substrates

The substrates were made of Al-1% Si and Al-1% Si-0.5% Cu alloys, with very similar mechanical behaviours. The gauge length of the samples for the tensile tests were 2.5 mm long, 1.8 mm wide and 1.4 mm thick, in the centre of a 'double bone' type sample. The surface was polished first by abrasive SiC paper (grade 1000, 1200), then by diamond paste (from 6 μm down to 0.25 μm) and finally by an alumina powder of 0.06 μm particle size. Between each stage of polishing, samples were carefully rinsed with water and ethyl alcohol and then submitted to an ultrasonic bath cleaning. Finally, these substrates were scratched in order to create a directional roughness (Fig. 1). Two scratching orientations were applied: longitudinal (on substrate Al-1% Si) and transversal (on substrate Al-1% Si-0.5% Cu) with respect to the tensile axis, and for each case two dimensions of roughness (0.25 μm and 1 μm) were chosen. Diamond paste with the corresponding particle size on cloth disks was used to carry out this scratching.

In the following, samples are identified as L 1 μm for longitudinal scratches done with 1 μm diamond paste granulometry, L 0.25 μm for longitudinal scratches with

0.25 μm granulometry, T 0.25 μm and T 1 μm for transverse scratches with the corresponding granulometries. One sample was kept as a reference with an isotropic fine roughness obtained by polishing down to 0.06 μm alumina, referred in the following as REF. (Fig. 2).

2.2. Film deposition

Silica films (SiO_2) were deposited on the aluminium alloy substrates by electron beam evaporation at 200°C. Thickness of the film was found to be 617 nm \pm 2%. Because of the thermal expansion mismatch between the substrate (23.6 10^{-6} $^\circ\text{K}^{-1}$ for the Al-Si alloys) and the film (0.5 10^{-6} $^\circ\text{K}^{-1}$ for the SiO_2 film), the deposition process induces compressive thermoelastic stresses in the film when cooling. Radius of curvature measurements have been performed on separate rectangular plate samples of the same SiO_2 on Al system. They gave compressive residual stresses for the SiO_2 films of 300 MPa, larger in absolute value than what can be expected from thermoelastic mismatch alone, and thus including an additional intrinsic compressive deposition stress.

2.3. Deformation experiment

In situ tensile experiments were performed in the S.E.M. on the above samples. The specific in situ tensile device, described in detail in Ref. [9], allowed the measurement of displacement and load variation during the straining. Because the straining system induces a symmetrical displacement of the grips with respect to the centre of the sample, the observation of the damage process does not need a systematic focusing and recovery of the image. For each system, observations are conducted in the central part of the sample where the strain will stay uniform during the tensile test, under a magnification of $\times 250$.

Beyond F the applied load and Δl the displacement, the crack density d in the film and ϵ the local longitudinal strain can be deduced from the SEM observations. The

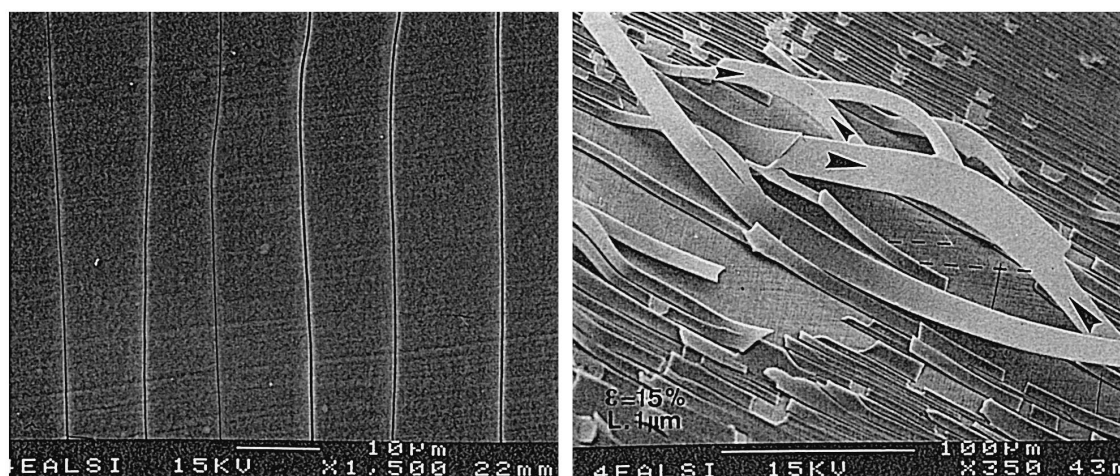


Fig. 3. Damage mechanisms developed during in situ straining. First: transverse cracking; then, debonding and buckling.

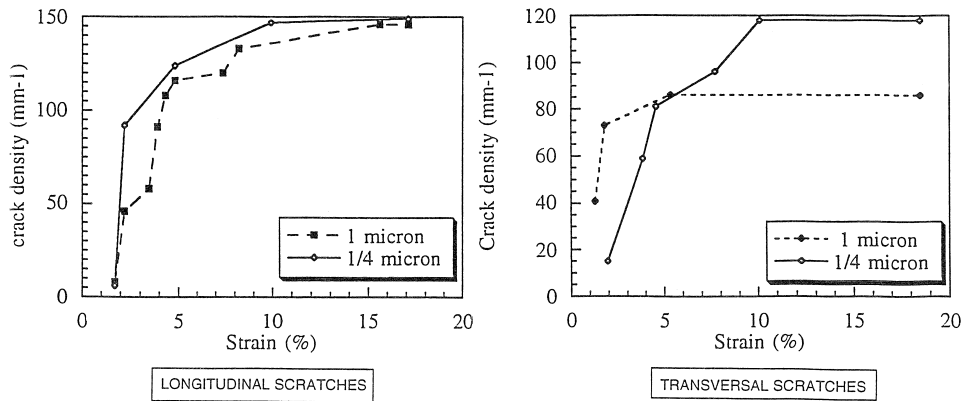


Fig. 4. Evolution of the transverse crack density with the tensile strain for transversal and longitudinal scratches.

local strain ϵ can be measured considering at the beginning of the straining a longitudinal segment L_0 marked by flaws on the surface. Then the length of this segment can be measured at different stages of the tensile test. A local longitudinal strain value is deduced by

$$\epsilon = \frac{L - L_0}{L_0} \quad (1)$$

where L is the length of the definite segment at different stages of the straining.

The evolution of the crack density d was evaluated using the same reference observations as above:

$$d = \frac{N}{L_0} \quad (2)$$

where N is the number of cracks on L_0 the initial length of the studied segment [10,11].

3. Results: Experimental

The experimental parameters defined previously allow characterization of the cracking evolution and the decohesion and buckling when debonding is observed (Fig. 3). The SEM in situ test allowed the observation of the mentioned damage progress, which can be characterized at different stages by critical strains. Typical transverse crack density evolutions are presented in Fig. 4. For each sample, the tensile test was conducted until the crack saturation was reached. Similar to experiments performed for

SiO₂ on copper systems [12], we observed that cracks in the film were normal to the tensile axis, irrespective of the scratch orientation and of the grain boundary orientations of the underlying grains in the substrate.

Table 1 summarizes the various damage process steps and the corresponding threshold strains for each type of specimens. In most cases, the decohesion and buckling of transverse film stripes occurred much before the crack saturation was achieved. Concerning the REF sample, a second cracking system appeared under the first one typically activated by the intergranular accommodation in the substrate at the interface. But we point out that no debonding was observed, even though the total strain exceeded 17%.

The error on the strain and on the crack density were evaluated at about $\pm 0.5\%$ and ± 4 cracks/mm respectively.

4. Results: decohesion energy calculations

A value of the interfacial cracking energy may be deduced from simple calculations in order to characterize the interfacial strength and allow comparisons between our samples. Let x , y and z be respectively the longitudinal (tensile) direction, the in-plane transverse direction and the normal to the sample plane. In the following, subindexes s and f correspond to the substrate and film, while indexes el or pl will refer to elastic or plastic (or total) strain components respectively.

Table 1

Summary of the damage behaviour of the SiO₂/Al–Si film on substrate systems for the various roughness characteristics

Specimens	REF.	L 0.25 μ m	L 1 μ m	T 0.25 μ m	T 1 μ m
Tensile strain for first transverse cracks (%)	1.9	2	1.3	2.1	1.3
Tensile strain for transverse crack saturation (%)	15.3	16	15	14.2	5.4
Transverse crack saturation density (mm ⁻¹)	(secondary crack system)	145	145	120	80
Tensile strain for decohesion and buckling of transverse film stripes (%)	(> 17)	4.8	4.3	7	1.3

The interfacial fracture energy G_i can be calculated using a combination of elastic fracture mechanisms and buckling theory of plates. G_i is determined by considering a relation assuming that the elastic energy stored in the film strip at the onset of debonding and buckling is equal to the buckling energy plus the Griffith interfacial crack propagation energy, as proposed by Evans and Hutchinson [13]:

$$G_i = (1 - \chi) \frac{h}{2E_f} (\sigma_{yy,f} - \sigma_{\text{buckling}}) \cdot \left(\sigma_{yy,f} - \frac{20a^2 - 3L^2}{4a^2 + L^2} \sigma_{\text{buckling}} \right) \quad (3)$$

where χ is a constant parameter ($\chi = 0.52$), E_f the Young modulus of the film. σ_{buckling} is the critical theoretical stress needed to buckle a free standing plate of the film with thickness h , L in width and $2a$ in length with clamped extremities [14]. $\sigma_{yy,f}$ is the compressive stress induced in the film by the transverse contraction of the substrate, during the tensile test, at the moment when buckling is observed experimentally. $\sigma_{yy,f}$, L and a are determined from the experiments. For $\sigma_{yy,f}$ determinations we assume that:

- the mechanical response of the film is fully elastic;
- the film/substrate system is constituted of isotropic materials;
- the stress components are null and the strain components are equal along y and z in the substrate;
- the film stiffness is negligible with regards to the mechanical behaviour of the substrate.

Both elastic and plastic strain of the substrate were considered to evaluate the strain transmitted to the film by the substrate, from which the stress in the film can be estimated. The substrate is submitted to an uniaxial longitudinal stress $\sigma_{xx,s}$. The elastic strains of the substrate in the x and y directions are:

$$\varepsilon_{xx,s}^{\text{el}} = \frac{\sigma_{xx,s}}{E_s} \text{ and } \varepsilon_{yy,s}^{\text{el}} = -\nu_s \frac{\sigma_{xx,s}}{E_s} \quad (4)$$

Because the observed failure processes (i.e., cracking and debonding) are observed at total strains of the substrate which widely exceed the elastic domain, the volume conservation of the sample may be written on the basis of

these total strains, nearly equal to the plastic strains, that is:

$$V = L_{x0} L_{y0} L_{z0} = L_{x0} L_{y0} L_{z0} (1 + \varepsilon_{xx,s}^{\text{pl}}) (1 + \varepsilon_{yy,s}^{\text{pl}})^2 \quad (5)$$

L_{0x} , L_{0y} and L_{0z} are the initial length, width and thickness of the sample. This relation allows calculation of the value of the transverse plastic strain of the substrate $\varepsilon_{yy,s}^{\text{pl}}$ from the longitudinal one $\varepsilon_{xx,s}^{\text{pl}}$ which is monitored both globally and locally during the test:

$$\varepsilon_{yy,s}^{\text{pl}} = \left(\frac{1}{1 + \varepsilon_{xx,s}^{\text{pl}}} \right)^{1/2} - 1. \quad (6)$$

As long as the film is adherent to the substrate, its transverse and longitudinal strains can be assumed to be identical to the total strains imposed by the substrate. Application of Hooke's law in the film then gives:

$$\sigma_{yy,f} = \frac{E_f}{1 - \nu_f^2} (\nu_f \varepsilon_{xx,f} + \varepsilon_{yy,f}) + \sigma_R \quad (7)$$

σ_R being the initial residual stress in the film.

From experimental determinations of total longitudinal strains of the substrate and average estimates of buckled zone dimensions, we calculated G_i with relation (3). The incertitude on G_i is estimated about $\pm 20\%$, mainly resulting from the wide distribution of values for $2a$ and L observable on a given specimen, and the incertitude on $\sigma_{yy,f}$. The results of the calculations are summarized in Table 2.

5. Discussion

The results in Table 1 do not show any significant difference between samples scratched at $0.25 \mu\text{m}$ with different orientations. Moreover these results are very similar to the values obtained for the reference system (sample REF) comparing the critical cracking onset strain and the crack density saturation strain. Then for a $0.25 \mu\text{m}$ depth of roughness scratches seem to present an influence only on the decohesion and buckling strain value, since the reference system with $0.06 \mu\text{m}$ roughness does not appear to debond.

Table 2

Experimental parameters corresponding to the observation of buckling, and determination of the apparent interfacial energy G_i by relation (3)

Specimens		REF.	L 0.25 μm	L 1 μm	T 0.25 μm	T 1 μm
Buckled zone dimensions						
Average values	$2a$ (μm)	None	12	11.4	14.6	25
	L (μm)	None	11.2	12.5	12.5	20.8
Critical buckling stress σ_{buckling} (MPa)		–	–781	–629	–639	–233
Experimental stress $\sigma_{yy,f}$ (MPa)		–	-1162 ± 83	-1007 ± 90	-1513 ± 86	-529 ± 88
G_i (J/m^{-2}) ($\sigma_R = 300\text{MPa}$)		larger	0.13	0.46	0.85	0.08

Considering now the $1\ \mu\text{m}$ scratched samples, the system with transverse scratches (sample $T\ 1\ \mu\text{m}$) show significant differences with sample $L\ 1\ \mu\text{m}$ —and actually with all other types of specimens. First cracking and decohesion and buckling almost appear simultaneously on sample $T\ 1\ \mu\text{m}$ at a 1.3% strain. The effect of the scratch orientation is important in that case. Transverse scratches seem to promote all processes of damage, and especially the debonding of the film.

Considering the interfacial crack energy estimations (Table 2), the major effect again appears to occur on the specimen $T\ 1\ \mu\text{m}$, with the lowest value of G_i . The REF sample shows the highest interfacial crack energy as suggested by the occurrence of a secondary transverse crack system (proving a good strain transfer from the substrate to the film), and no decohesion observed even at high strain.

Experimental evidence shows in our case that an increase of interfacial roughness does not seem to produce an increase of interfacial fracture toughness (see Fig. 5), contrary to the most current observations and models [15,16]. This embrittling effect with increasing interfacial roughness depends on both the amplitude and direction of the interfacial asperities: it is less obvious for longitudinal or transverse $0.25\ \mu\text{m}$ asperities and only enhances the film decohesion. But it becomes more effective to enhance transverse cracking of the film for longitudinal $1\ \mu\text{m}$ asperities, and above all to induce much easier decohesion of the film transverse stripes for transverse $1\ \mu\text{m}$ asperities.

Recalling that the thickness of the SiO_2 layers on our specimens is about $0.6\ \mu\text{m}$; indeed, it may be expected

that the effect of interfacial asperities on the local short range stress fields concentrations around these asperities becomes more critical when the roughness amplitude is more than the film thickness itself. Then the interfacial roughness seems to be a critical factor for nucleation of interfacial cracks.

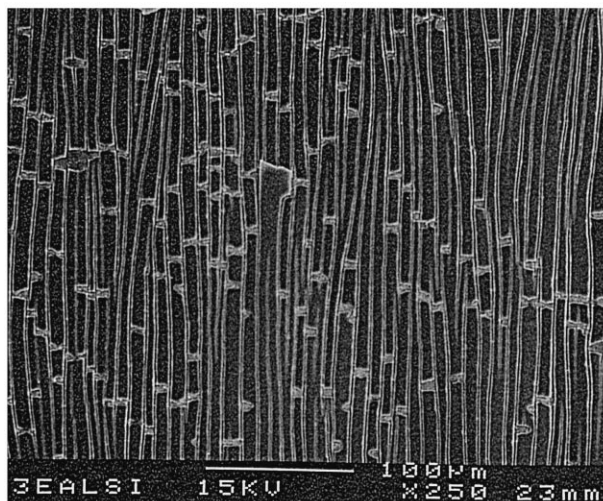
Besides, concerning the propagation of these interfacial cracks, it must be noted that the scratches which are transverse to the tensile direction are actually parallel to the interfacial crack propagation direction when transverse film stripes debond and buckle. Longitudinal scratches are perpendicular to the crack propagation direction, and might make this propagation more difficult.

These considerations may form the bases for an explanation of the observed differences in film stability and apparent interfacial crack energy, but a detailed analysis of the influence of the direction of the interfacial asperities on the mode mixity of the interfacial cracks appears to be necessary, both at the crack nucleation stage and during the crack propagation.

6. Conclusions

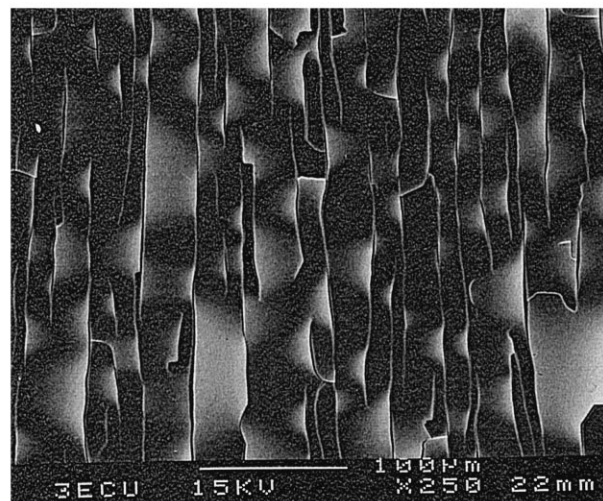
In situ tensile experiments on film on substrate samples presenting different types of interfacial roughness were performed. The experiments allowed us on one hand to observe the evolution of damage (film cracking and debonding), on the other hand to correlate the damage evolution to the various kinds of mechanically induced interfacial roughness.

15%



LONGITUDINAL SCRATCHES $1/4\ \mu\text{m}$

5%



TRANSVERSAL SCRATCHES $1\ \mu\text{m}$

Fig. 5. Typical damage observed when reaching crack saturation and debonding (S.E.M.). Debonded areas for the samples with longitudinal $0.25\ \mu\text{m}$ scratches are much smaller than those with transverse $1\ \mu\text{m}$ scratches. The dimensions of the buckled zones of the cracked film strips allow critical buckling stress calculation and thus crack propagation energy estimation. The numbers on top of the micrograph indicate the tensile strain reached when the observation was made.

The following main points may be retained:

(i) The interfacial roughness promotes the film cracking;
(ii) The direction of the surface scratches with respect to the tensile axis controls the activation of the successive steps of damage:

- the samples with transverse scratches showed a tendency to activate the cracking of the film at lower strains than the samples with longitudinal scratches.
- the interfacial cracking and debonding process showed the same tendency. These effects were enhanced for the samples with steeper scratches.

(iii) The values of the critical adhesion parameters deduced from the experiments were consistent with the observations, with lower apparent interfacial fracture energy values for the samples showing cracking and debonding at lower strain.

Finally we suggest that further experiments may involve directional asperities with more precise and regular geometrical characteristics, for instance by machining a polished surface with help of a nanoindenter, to obtain test substrate areas with well defined scratches with varying amplitudes, wavelength and orientation, even possibly on the same tensile specimen.

References

- [1] M.S. Hu, A.G. Evans, *Acta Met.* 37 (1989) 917–925.
- [2] A.G. Evans, B.J. Dalgleish, *Acta Met.* 40 (1992) S295–S306.
- [3] T. Ye, Z. Suo, A.G. Evans, *Int. J. Solids Struct.* 29 (1992) 2639–2648.
- [4] Z. Suo, J.W. Hutchinson, *Mat. Sci. Eng. A107* (1989) 135–143.
- [5] D. Tabor, *J. Colloid Interface Sci.* 58 (1) (1977) 2–13.
- [6] K.S. Chan, *Met. Trans. A* 22 (1991) 2021–2029.
- [7] D.E. Savage, N. Schimke, Y.H. Phang, M.G. Lagally, *J. Appl. Phys.* 71 (7) (1992) 3283–3293.
- [8] J.D. Jero, R.J. Kerans, *Scr. Met. Mater.* 24 (1990) 2315–2318.
- [9] M. Ignat, *Key Eng. Mater.* 116–117 (1996) 279–290.
- [10] P. Scafidi, Doctorate Thesis, I.N.P. de Grenoble, France 1995.
- [11] P. Scafidi, M. Ignat, M. Dupeux, *Mat. Res. Soc. Symp. Proc.* 309 (1993) 55–60.
- [12] D.C. Agrawal, R. Raj, *Acta Met.* 37 (1989) 1265–1270.
- [13] A.G. Evans, J.W. Hutchinson, *Int. J. Solids Struct.* 40 (1984) 455–466.
- [14] S.P. Timoshenko, J.M. Gere, *Theory of Elastic Stability*, 2nd edn., McGraw-Hill, New York, 1961.
- [15] A.G. Evans, J.W. Hutchinson, *Acta Met.* 37 (1) (1989) 906–916.
- [16] A.G. Evans, M. Rühle, B.J. Dalgleish, P.G. Charalambides, *Met. Trans. A* 21A (1990) 2419–2429.